

Small Molecule Targets Env for Endoplasmic Reticulum-Associated Protein Degradation and Inhibits Human Immunodeficiency Virus Type 1 Propagation[∇]

Alenka Jejcic,¹ Robert Daniels,² Laura Goobar-Larsson,¹ Daniel N. Hebert,² and Anders Vahlne^{1*}

Department of Laboratory Medicine, Division of Clinical Microbiology, Karolinska Institutet, Stockholm, SE-141 86, Sweden,¹ and Department of Biochemistry and Molecular Biology, Program in Molecular and Cellular Biology, University of Massachusetts, Amherst, Massachusetts 01003²

Received 10 August 2008/Accepted 16 July 2009

Human immunodeficiency virus type 1 (HIV-1) is dependent on its envelope glycoprotein (Env) to bind, fuse, and subsequently infect a cell. We show here that treatment of HIV-1-infected cells with glycyL-prolyl-glycine amide (GPG-NH₂), dramatically reduced the infectivity of the released viral particles by decreasing their Env incorporation. The mechanism of GPG-NH₂ was uncovered by examining Env expression and maturation in treated cells. GPG-NH₂ treatment was found to affect Env by significantly decreasing its steady-state levels, its processing into gp120/gp41, and its mass by inducing glycan removal in a manner dependent on its native signal sequence and the proteasome. Therefore, GPG-NH₂ negatively impacts Env maturation, facilitating its targeting for endoplasmic reticulum-associated protein degradation, where Env is deglycosylated en route to its degradation. These findings illustrate that nontoxic drugs such as GPG-NH₂, which can selectively target glycoproteins to existing cellular degradation pathways, may be useful for pathogen therapy.

The endoplasmic reticulum (ER) contains a number of molecular chaperones and folding factors that aid in the maturation of proteins that traverse the secretory pathway. This process is strictly monitored by the ER quality control system, which selects properly folded proteins for export to the Golgi (16) and targets misfolded proteins for destruction through the ER-associated protein degradation pathway (ERAD) (4, 28). Once an ER protein is selected as a substrate for ERAD, it is translocated from the ER lumen to the cytosol through an ER translocon. This retrotranslocation process is thought to be driven by either the cytosolic AAA-ATPase p97 (39) or the 19S proteasome cap (23). Upon entrance into the cytosol, the ERAD substrate is ubiquitinated, and its glycans are removed by an N-glycanase to prepare it for proteasomal degradation (11, 28).

Viral envelope glycoproteins utilize the host cell secretory pathway for their proper maturation and trafficking to the site of viral assembly. The human immunodeficiency virus type 1 (HIV-1) encodes the envelope glycoprotein (Env), which initiates HIV-1 infections by mediating attachment and fusion of the viral envelope with the host cell membrane (17). Therefore, infectious HIV-1 particle production relies on the ability of Env to pass the rigorous ER quality control system.

Env is initially synthesized as a type I membrane precursor glycoprotein termed gp160, which is cotranslationally targeted to the ER by its 30-amino-acid N-terminal signal sequence (24). Within the ER, gp160 receives ~30 N-linked glycans and is assisted in its maturation by the chaperones BiP, calnexin, and calreticulin as it undergoes extensive disulfide bond formations (15, 21, 31). Once gp160 has reached its native state

with ten disulfide bonds and its signal sequence has been cleaved posttranslationally (21, 25), it assembles into trimers (26) and is exported to the Golgi. Within the Golgi, gp160 is cleaved by cellular endoproteases, yielding the transmembrane protein gp41 and the noncovalently associated surface protein gp120 (27). Thereafter, this complex is transported to the plasma membrane, where it is incorporated into the envelope of assembling HIV-1 particles.

We have previously shown that a tripeptide amide corresponding to a conserved motif of the HIV-1 Env, glycyL-prolyl-glycine amide (GPG-NH₂), suppressed the replication of all 47 HIV-1 laboratory strains and clinical isolates examined with a 50% inhibitory concentration of ~10 μM, a concentration that is 200- to 2,000-fold less than what affected cell growth or had other toxic effects on peripheral blood mononuclear cells (35). However, this suppression was not, as we had anticipated, due to interactions of the peptide with the early events of the HIV-1 replication cycle, such as attachment or entry (36). In the present study, we demonstrate that GPG-NH₂ reduced Env incorporation into HIV-1 particles during replication by targeting Env toward the ERAD pathway. The ability of GPG-NH₂ to target Env for degradation was dependent on the presence of functional proteasomes and required the full-length Env signal sequence. These findings illustrate that small molecules may be utilized therapeutically to specifically target unwanted pathogenic proteins for degradation by the existing cellular machinery.

MATERIALS AND METHODS

Reagents and antibodies. GlycyL-prolyl-glycine amide (GPG-NH₂) and glycyL-prolyl-glycine (GPG-OH) were purchased from Bachem Feinchemikalien. The antibody to gp160/41 (Chessie 8) (1) was obtained through the NIH AIDS Research and Reference Reagent Program. Calnexin and LAMP-1 antibodies were obtained from Santa Cruz Biotechnology and BD Biosciences, respectively. Additional antibodies to gp160/gp120 (F58/V3 and p4/D10) and p24 were pre-

* Corresponding author. Mailing address: Department of Laboratory Medicine, Division of Clinical Microbiology, Karolinska Institutet, Stockholm, SE-141 86, Sweden. Phone: 46 8 5858 1313. Fax: 46 8 5858 7933. E-mail: anders.vahlne@ki.se.

[∇] Published ahead of print on 29 July 2009.

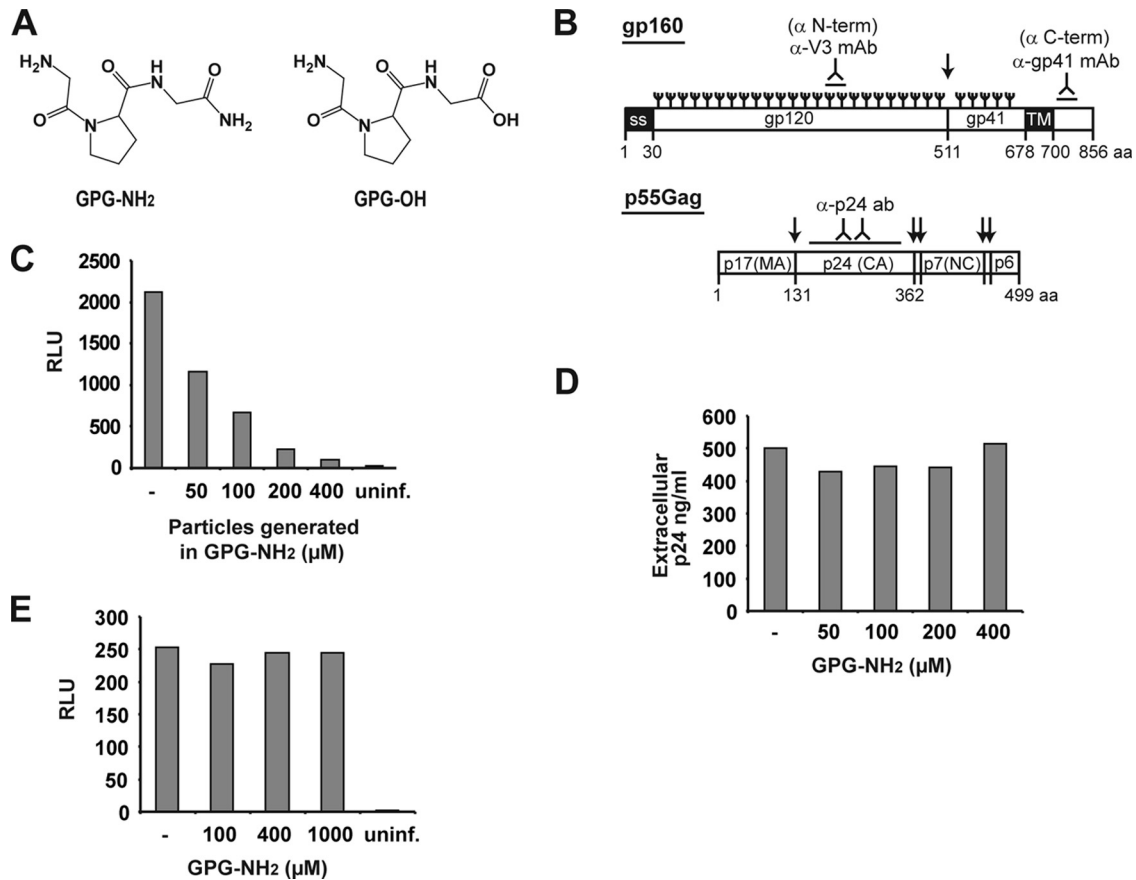


FIG. 1. GPG-NH₂ treatment reduces HIV-1 particle infectivity. (A) Structure of GPG-NH₂ and GPG-OH. (B) Linear structures of the HIV-1 Env precursor protein (gp160) and the precursor protein p55Gag depicting antibody recognition sites (inverted “Y”), N-linked glycans (trident symbol), and proteolytic cleavage sites (↓). (C) HIV-1 particles were produced in the indicated concentrations of GPG-NH₂. Equivalent p24 amounts of the viral particles were used to infect TZM-bl cells at 4°C for 2 h, the infection medium was removed, and the cells were cultured for 48 h in the presence of 5 μM indinavir. The luciferase activity in the lysates was monitored to determine the relative infectivity of the particles. (D) ACH-2 cells were pretreated with 0 to 400 μM GPG-NH₂ for 24 h before HIV-1 replication was induced with PMA for 48 h. HIV-1 particle production was determined by measuring the extracellular p24 by ELISA. (E) HIV-1 virus was mixed with 0 to 1,000 μM GPG-NH₂ and incubated with TZM-bl cells for 2 h. Upon removal of the infection media the cells were incubated in the presence of 5 μM indinavir for 48 h. The cells were subsequently harvested, and the infectivity was determined by measuring the intracellular luciferase activity.

viously described (8, 13). Peroxidase-conjugated concanavalin A was obtained from Sigma.

Cell lines and plasmids. HeLa-tat III, ACH-2, SupT1, and TZM-bl cell lines (10, 12, 34, 37) and the infectious HIV-1 expressing plasmid pNL4-3 (3) were obtained through NIH AIDS Research and Reference Reagent Program. The expression plasmids for Env from the HIV-1 strain NL43 (pNL1.5EU) (32) and for Rev (pBRev) were kindly provided by S. Schwartz (Uppsala University, Uppsala, Sweden). ΔnSS-gp160 was created from pNL1.5EU by mutating the start codon ATG to ATA. PCR^R3.1/CAT expresses chloramphenicol acetyltransferase (CAT) and was purchased from Invitrogen.

Virus expression and precipitation of HIV-1 particles. ACH-2 cells (8×10^5 cells/ml) were cultured with or without GPG-NH₂ or GPG-OH for various time prior to the addition of 100 nM 12-phorbol-13-myristate acetate (PMA). Three days later, the cell culture supernatants were collected, cleared by centrifugation at $300 \times g$ for 10 min, passed through 0.45-μm-pore-size filters, and the particles were precipitated at 4°C for 48 h in 1:6 (vol/vol) with 40% polyethylene glycol 6000 containing 0.667 M NaCl. The precipitated particles were allowed to sediment at $16,000 \times g$ for 20 min at 4°C. The virus pellets were then dissolved in radioimmunoprecipitation assay (RIPA) buffer containing 50 mM Tris-HCl (pH 7.4), 1% Triton X-100, 1% deoxycholate, 150 mM NaCl, 1 mM EDTA, and 0.1% sodium dodecyl sulfate (SDS) and supplemented with Complete protease inhibitor cocktail (Roche).

Infectivity assay and syncytia formation. For the infectivity assay, 2×10^5 TZM-bl cells were infected with virus equivalent to 200 ng of p24 in 0.5 ml of

culture medium. After 2 h at 4°C, the infection medium was replaced with virus-free culture medium containing 5 μM indinavir. The cells were harvested after 40 h at 37°C and assayed for luciferase activity using the Bright-Glo luciferase assay system (Promega). To test for syncytium formation, ACH-2 cells were cultured in 10 μM indinavir with or without 1,000 μM GPG-NH₂. After 24 h, 250,000 SupT1 cells were added to and cocultured with 20,000 ACH-2 cells. Syncytium formation was then monitored by light microscopy 24 and 40 h later.

Transfection, drug treatments, and immunoblotting. HeLa-tat III cells ($\sim 5 \times 10^5$ cells/dish) were treated with the indicated concentrations of GPG-NH₂ prior to cotransfection with the CAT expressing control plasmid and the appropriate construct using FuGENE 6 (Roche). For inhibition of the proteasome (lactacystin [LCT] and epoxomicin), glucosidases (castanospermine [CST]), and mannosidases (deoxymannojirimycin [DMJ] and kifunensine [KIF]), the drugs were added to the cells at 8 to 12 h posttransfection. The isolated virus and cells were lysed in RIPA buffer, standardized to p24 or CAT levels, resolved by SDS-polyacrylamide gel electrophoresis (PAGE), transferred to nitrocellulose membranes, and immunoblotted. The membranes were exposed to film for the appropriate time, and band intensities were quantified by using GeneTools analysis software (SynGene).

UPR, enzyme-linked immunosorbent assay (ELISA), and measurement of RT activity. Induction of unfolded protein response (UPR) after GPG-NH₂ treatment was examined by assaying XBP-1 mRNA splicing as previously described (22). In brief, HeLa-tat III cells were exposed to 5 mM dithiothreitol (DTT) for 3 h or 0 to 1 mM GPG-NH₂ for 48 h. The total cellular RNA was isolated by

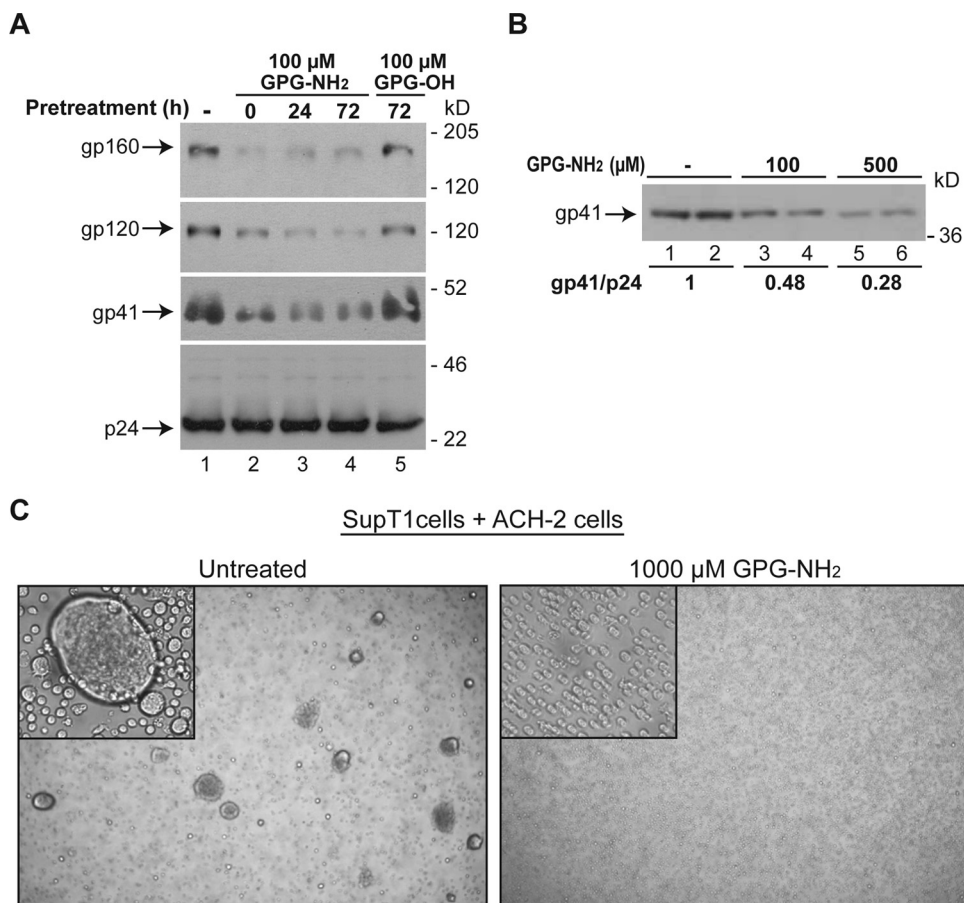


FIG. 2. GPG-NH₂ reduces incorporation of Env into HIV-1 particles. (A) ACH-2 cells were pretreated with GPG-NH₂ or GPG-OH for the indicated times before induction with PMA for 72 h. The particles were isolated from the extracellular medium by polyethylene glycol precipitation, lysed, separated by SDS-PAGE, immunoblotted, and probed with the α-V3 monoclonal antibody (which recognizes gp120 and gp160), the α-gp41 monoclonal antibody (which recognizes gp41 and gp160), and p24 antiserum. (B) Immunoblot showing the amount of gp41 present in polyethylene glycol-precipitated HIV-1 particles produced by HeLa-tat III cells. The cells pretreated for 20 h with the indicated concentrations of GPG-NH₂ prior to transfection with the infectious clone, pNL3-4. The viral particles were isolated 72 h posttransfection and standardized to the extracellular p24 concentrations measured by ELISA. The gp41/p24 ratio was calculated by densitometry. (C) Light microscopy photos of syncytium formation between ACH-2 and CD4-positive SupT1 cells with insets showing higher magnification images. The ACH-2 cells were pretreated for 24 h with 10 μM indinavir and the indicated concentrations of GPG-NH₂ prior to PMA stimulation. Five hours later the SupT1 cells were added to the ACH-2 cells, which were then cocultured for 40 h.

using an RNeasy isolation kit (Qiagen). Standard reverse transcriptase PCR (RT-PCR) was performed by using the oligonucleotide mXBP1 804AS, followed by amplification of spliced or unspliced XBP-1 by PCR with the primers 804AS XBP1 and 383S XBP as previously described (22).

The p24 levels or RT activity in cell culture supernatants were quantified by using p24-ELISA (18) or a Lenti-RT activity assay (Cavidi Tech), respectively. CAT concentrations in cell lysates were quantified by using the CAT ELISA kit (Roche).

Subcellular fractionation and alkaline extraction. Cell membrane fractions were prepared from HeLa-tat III cells homogenized with a Dounce homogenizer in 10 mM HEPES (pH 7.4), 1 mM EDTA, and 0.25 M sucrose supplemented with 125 μM phenylmethylsulfonyl fluoride and 2.5 μg of aprotinin and leupeptin/ml. Nuclei and nondisrupted cells were removed by centrifugation at 1,500 × g for 10 min at 4°C. The supernatants were further centrifuged at 180,000 × g for 1 h at 4°C to separate the membrane vesicles from cytosolic components. The supernatants were precipitated with 15% trichloroacetic acid, and the precipitates rinsed in acetone and dissolved in reducing sample buffer. The membrane pellets were resuspended in 0.5 mM sucrose containing 50 mM TEA (pH 7.5) and 1 mM DTT. For isolation of integral membrane proteins by alkaline extraction, the microsome suspension was first diluted 20 times in 0.1 M NaCO₃ (pH 11.5), incubated for 30 min on ice, and then separated through a 0.5 M sucrose cushion for 1 h at 180,000 × g at 4°C. The pellets were resuspended in reducing

sample buffer, while the supernatants were precipitated with trichloroacetic acid as described above.

PNGase F and Endo H digestion. Cell lysates in RIPA buffer were supplemented with 0.5% SDS and 1% β-mercaptoethanol and denatured for 10 min at 100°C. The PNGase F reactions were adjusted to 1% NP-40, and the Endo H (endo-β-N-acetylglucosaminidase H) reactions were adjusted to 50 mM sodium citrate (pH 5.5). Incubation followed at 37°C for 1 h with 16 U per μl of lysate of PNGase F or Endo H (New England Biolabs).

RESULTS

GPG-NH₂ decreases HIV-1 particle infectivity. Initially, the effects of GPG-NH₂ (the structure is depicted in Fig. 1A) on infectious HIV-1 particle production was examined. HIV-1 was generated from chronically infected ACH-2 cells in the absence or presence of GPG-NH₂. TZM-bl cells, which express luciferase from an HIV-1 Tat-dependent promoter, were then infected with equivalent amounts of the produced viral particles as determined by p24 levels. The infectivity of HIV-1

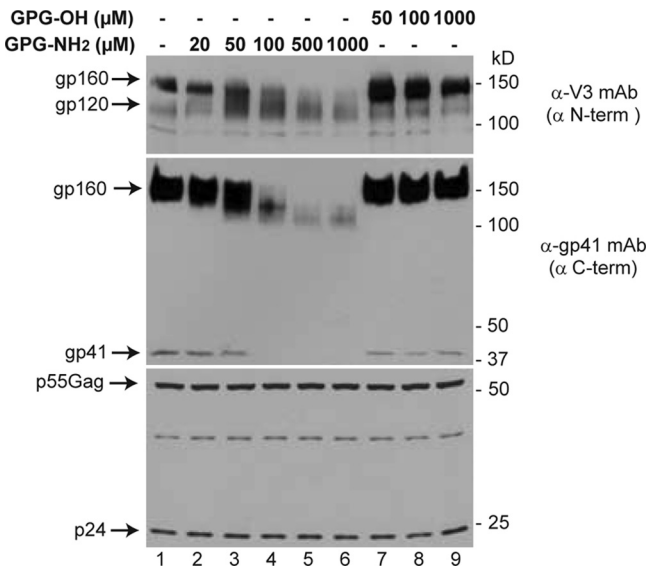


FIG. 3. GPG-NH₂ caused a decrease in gp160 mobility and steady-state levels. HeLa-tat III cells were transfected with plasmids expressing either gp160 or p55Gag and cultured in the indicated concentrations of GPG-NH₂ or GPG-OH for 20 h (gp160) or 48 h (p55Gag). After harvesting, the cell lysates were separated by SDS-PAGE and immunoblotted with antibodies to the N terminus of gp160, α-V3 (upper panel); the C terminus of gp160, α-gp41 (middle panel); or p55Gag/p24 (bottom panel).

particles produced in 50 μM GPG-NH₂ was ~50% of those generated in the absence of GPG-NH₂ (Fig. 1C), and it declined in a dose-dependent fashion. However, GPG-NH₂ treatment did not affect HIV-1 particle production, since the extracellular viral capsid protein (p24) levels and the viral RT activity were comparable to the untreated samples (Fig. 1D and data not shown). To address whether GPG-NH₂ decreased viral infectivity by inhibiting viral binding and entry, TZM-bl cells were infected with untreated virus in the presence of

GPG-NH₂. Even at 1,000 μM, GPG-NH₂ showed no effect on luciferase expression, indicating that the drug does not prevent viral binding and entry (Fig. 1E). Together, these findings indicate that HIV-1 particles, produced in the presence of GPG-NH₂, are less infectious due to inhibition of a step in the replication process that occurs after entry.

GPG-NH₂ treatment reduces Env incorporation into HIV-1 particles. The decreased infectivity of HIV-1 particles, produced in the presence of GPG-NH₂, could be due to a reduced ability of the virus to enter target cells. Since HIV-1 entry into cells is mediated by Env, its content in the particles was examined. ACH-2 cells were treated with 100 μM GPG-NH₂ for various times prior to stimulating virus production with PMA. As controls, ACH-2 cells were either untreated or pretreated with the inactive analog GPG-OH (the structure is depicted in Fig. 1A). At 3 days postinduction, the viral particles were collected and examined for the incorporation of p24, unprocessed Env (gp160), and processed Env (gp120/gp41) by immunoblotting (Fig. 2A). In the presence of GPG-NH₂ the particle incorporation of gp160, gp120, and gp41 decreased by 60 to 80% compared to the controls, whereas the p24 levels remained unaffected (Fig. 2A, compare lanes 1 and 5 to lanes 2 to 4).

To determine whether GPG-NH₂ reduced the viral incorporation of Env in a cell-type-specific manner, HIV-1 particles produced by the human epithelial derived cell line HeLa-tat III were examined. The cells were untreated or treated with various amounts of GPG-NH₂ 20 h prior to transfection with the HIV-1 infectious clone, pNL4-3. The viral particles were collected 3 days posttransfection and standardized to p24 levels by ELISA (data not shown). Similar to ACH-2 cells, GPG-NH₂ treatment reduced the incorporation of gp41 into the particles produced by HeLa-tat III cells (Fig. 2B). This effect appeared to be dose dependent since the gp41/p24 ratio decreased from 0.48 to 0.28 in the presence of 100 and 500 μM GPG-NH₂, respectively (Fig. 2B, compare lanes 1 and 2 to lanes 3 to 6). Decreased levels of processed Env (gp120/gp41) on the viral

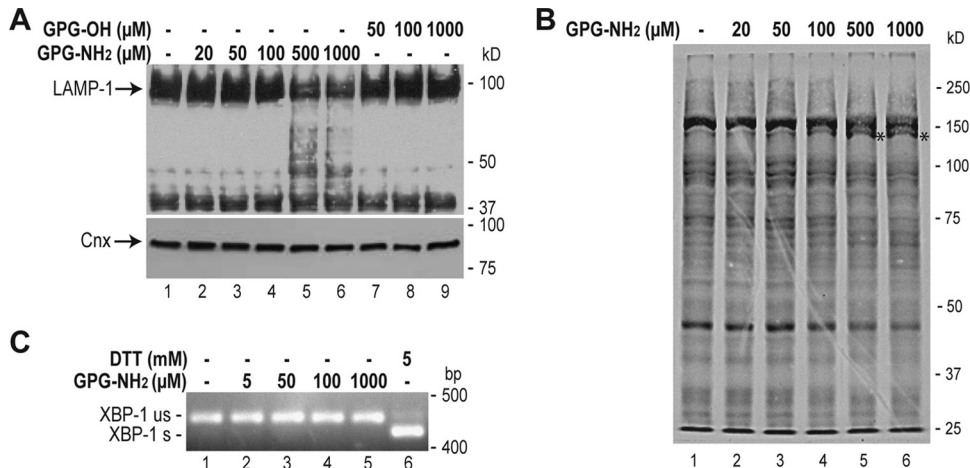


FIG. 4. GPG-NH₂ affects glycoproteins. (A) Immunoblots of HeLa-tat III cells treated for 48 h as indicated and probed with antibodies to LAMP-1 (upper panel) and calnexin (bottom panel). (B) Glycoprotein blot of HeLa-tat III cell lysates collected from cells cultured in the indicated concentrations of GPG-NH₂ for 48 h and probed with concanavalin A. (C) RT-PCR analysis of XBP-1 mRNA splicing using RNA templates from HeLa-tat III cells treated for 48 h with the indicated concentrations of GPG-NH₂ or for 3 h with the UPR inducer DTT. The unspliced and spliced XBP-1 mRNAs are designated by “us” and “s,” respectively.

surface should reduce the capacity of the virus to bind to and fuse with the target cells. To examine this, we developed a cell model that is based on the ability of infected cells, which express gp120/gp41 on their surface, to fuse with uninfected viral target cells. This fusion results in the formation of large multinuclear cells, called syncytia, which can easily be monitored under a light microscope. ACH-2 cells express gp120/gp41 on their surface, but due to their lack of CD4 expression they cannot form syncytia among themselves. Thus, the ACH-2 cells were used as “virus” since they must be cocultured with CD4-positive target cells to form syncytia. The ACH-2 cells were either untreated or pretreated for 24 h with 1,000 μ M GPG-NH₂. In addition, the cell cultures were treated with 10 μ M indinavir, an HIV-1 protease inhibitor, to prevent production of infectious virus. The ACH-2 cells were subsequently stimulated with PMA, to increase the cell surface levels of Env, 5 h prior to the addition of the CD4 positive cells, SupT1. After 24 and 40 h, a significant number of large syncytia had been formed in the GPG-NH₂-untreated cocultures, but none were detected in those containing the GPG-NH₂-pretreated ACH-2 cells (Fig. 2C). Together, these findings show that GPG-NH₂ does not inhibit intact HIV-1 particles from fusing with target cells but rather that HIV-1 particles produced in the presence of GPG-NH₂ have a decreased incorporation of gp120 and gp41. This reduces the ability of the HIV-1 particles to fuse with target cells and thus decreases their infectivity.

GPG-NH₂ decreases the steady-state levels and mass of gp160. To examine the mechanism by which GPG-NH₂ reduced Env incorporation into HIV-1 particles and prevented the ACH-2 cells from fusing with the CD4 positive SupT1 cells, the intracellular expression of Env was studied in a noninfectious system. HeLa-tat III cells were treated with various concentrations of GPG-NH₂ or GPG-OH 20 h prior to the transient expression of gp160 and the internal control protein, CAT. The cells were collected 20 h posttransfection, and the lysates were standardized to the CAT levels, separated by SDS-PAGE, and immunoblotted for Env. Antibodies to the N-terminal region of gp160 and gp120 (see Fig. 1B) revealed a GPG-NH₂ dose-dependent increase in gp160 mobility that coincided with decreases in its steady-state levels (Fig. 3, upper panel, lanes 1 to 6). Since the gp160 mobility change was not discernible from processing to gp120, a C-terminal antibody that recognized gp160 and gp41 was utilized (see Fig. 1B). This antibody revealed a GPG-NH₂-dependent increase in gp160 mobility and a decrease in its steady-state levels, as well as a reduction in its processing to gp41 (Fig. 3, middle panel, lanes 1 to 6). Given that the smaller gp160 species were observed with antibodies to both termini, at GPG-NH₂ concentrations inhibiting its cleavage to gp41, enhanced processing of Env to gp120 and gp41 was ruled out as the cause of the increased gp160 migration.

Unlike the heavily glycosylated gp160, the steady-state levels of the HIV-1 cytosolic precursor protein p55Gag and its cleavage product p24 were unaffected by GPG-NH₂ treatment (Fig. 3, bottom panel). These results suggested that GPG-NH₂ reduced Env levels in HIV-1 particles by interfering with gp160 biosynthesis rather than by inhibiting its incorporation during the process of viral assembly.

GPG-NH₂ has higher specificity for the HIV-1 glycoprotein than for cellular glycoproteins. Since GPG-NH₂ did not alter

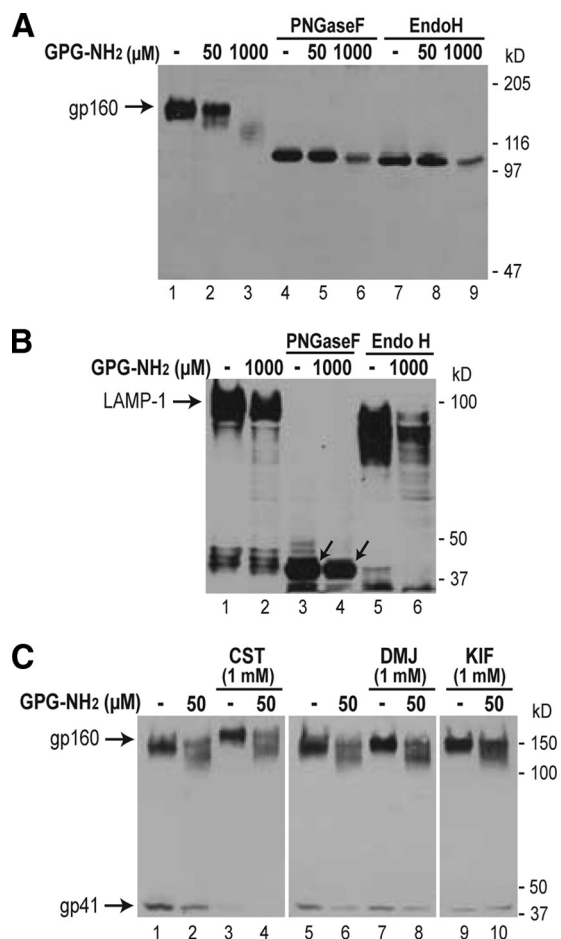


FIG. 5. GPG-NH₂ decreases the number of glycans on gp160. (A) Immunoblots of cell lysates prepared from HeLa-tat III cells cultured in the indicated concentrations of GPG-NH₂, harvested 20 h posttransfection with gp160, and probed with gp41 antibodies. Where indicated, the lysates were subjected to deglycosylation by PNGaseF or Endo H prior to analysis. (B) HeLa-tat III cells cultured for 48 h in the presence of the indicated GPG-NH₂ concentration were harvested and subjected to deglycosylation as in panel A, followed by immunoblotting against LAMP-1. Bands representing fully deglycosylated LAMP-1 are highlighted by arrows. (C) gp160-transfected HeLa-tat III cells were cultured in the indicated concentrations of GPG-NH₂ and treated with the glucosidase inhibitor CST and the mannosidase inhibitors DMJ and KIF at 8 h posttransfection. The lysates were harvested 10 h later and subjected to immunoblotting against gp41.

the expression or processing of the cytosolic viral precursor protein p55Gag, it was further explored whether GPG-NH₂ had a general or selective effect on proteins within the secretory pathway. First, the effects of GPG-NH₂ were examined on the endogenously expressed glycoprotein LAMP-1 (lysosome-associated membrane protein 1), which, like gp160, is a heavily glycosylated type 1 membrane protein. A slight reduction in its steady-state levels and increased mobility was observed at 500 μ M GPG-NH₂ (Fig. 4A, upper panel, lanes 5 and 6). This concentration is ~25-fold higher than what is required for similar effects on gp160. Next, the endogenous nonglycosylated type 1 ER membrane protein calnexin was examined and found to be completely unaffected by GPG-NH₂ treatment (Fig. 4A, lower panel). To investigate whether GPG-NH₂ has

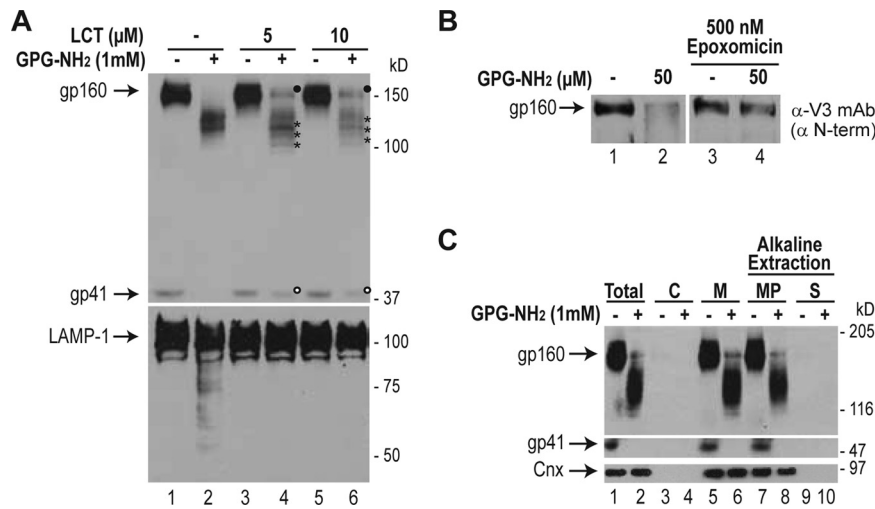


FIG. 6. GPG-NH₂ requires functional proteasomes to target gp160 for ERAD. (A) gp160-transfected HeLa-tat III cells were cultured in the indicated concentration of GPG-NH₂ and treated with the proteasome inhibitor LCT at 12 h posttransfection. The cells were harvested 10 h later, lysed, separated by SDS-PAGE, and immunoblotted against gp41 (upper panel) or LAMP-1 (bottom panel). Note, in the presence of LCT, the fully glycosylated gp160 (●), the processing to gp41 (○), and the stabilized deglycosylated lower-molecular-weight species (*). (B) gp160-transfected HeLa-tat III cells were cultured in the indicated concentrations of GPG-NH₂ and treated with the proteasome inhibitor epoxomicin as described in panel A and immunoblotted against the N terminus of gp160 (α-V3). (C) GPG-NH₂-treated HeLa-tat III cells expressing gp160 were homogenized at 20 h posttransfection and fractionated. Immunoblots against gp160/gp41 and calnexin performed on equal fractions from the total homogenate (Total) after removal of the nuclei and nondisrupted cells, the cytosol (C), or the homogenate supernatant that remained after removal of the cellular membranes (M) are shown. The cellular membranes were then subjected to alkaline extraction to separate the integral membrane proteins (MP) from the soluble or peripherally attached proteins (S).

a general effect on glycoproteins, the glycoprotein expression profile in the HeLa-tat III cells was analyzed with the lectin, concanavalin A. Similar to LAMP-1, the cellular glycoprotein pattern was only slightly altered at the highest GPG-NH₂ concentrations (500 to 1,000 μM), where the steady-state levels showed a minor decrease and a high-molecular-mass glycoprotein band of ~150 kDa appeared to increase in mobility (Fig. 4B, lanes 5 and 6). These results indicated that GPG-NH₂ has a significantly higher selectivity for gp160 than cellular glycoproteins.

During HIV-1 infection the majority of gp160 resides within the ER (21). The high proportion of gp160 within the ER and the observation that GPG-NH₂ reduces its steady-state levels raised the possibility that GPG-NH₂ induced ER stress. The induction of ER stress activates the UPR, which could facilitate enhanced degradation of gp160, resulting in the observed decrease in its steady-state levels. The UPR was followed by monitoring splicing of the XBP-1 mRNA. In contrast to the known UPR inducer, dithiothreitol (DTT), GPG-NH₂ treatment of HeLa-tat III cells did not activate the UPR, even at concentrations up to 1 mM for 48 h (Fig. 4C, compare lane 6 to lanes 1 to 5). Therefore, the ability of GPG-NH₂ to decrease gp160 steady-state levels was not a result of UPR activation.

GPG-NH₂ treatment alters the glycan status of gp160 prior to Golgi transport. Apart from proteolysis, the heterogeneous mass reduction of gp160 after GPG-NH₂ treatment could be caused by N-glycan removal or deficient glycosylation. To examine these possibilities, whole-cell lysates were treated with the N-glycanase PNGase F or Endo H. After deglycosylation with either glycanase, gp160 produced in the absence or presence of GPG-NH₂ coalesced as single bands with identical mobility (Fig. 5A, compare lanes 1 to 3 to lanes 4 to 9). This

demonstrated that the reduced mass of gp160 was not caused by proteolysis but was due to variations in its carbohydrate content. Furthermore, the complete deglycosylation of gp160 by Endo H indicated that gp160 had not been exported to the medial Golgi, where complex carbohydrates are added that prevent Endo H deglycosylation.

Similar to gp160, deglycosylation of LAMP-1 with PNGase F resulted in single sharp bands with equal mobilities, regardless of GPG-NH₂ treatment (Fig. 5B). However, LAMP-1 exhibited resistance to Endo H digestion, demonstrating that its transport to the Golgi is not affected by GPG-NH₂ treatment. This indicated that the higher sensitivity of gp160 toward GPG-NH₂ may be due to its longer residence within the ER.

N-linked glycans are trimmed of glucoses and some mannoses before they exit the ER for the Golgi. To determine whether glycan trimming was required for GPG-NH₂ to affect gp160, the glucosidase I and II inhibitor CST or the mannosidase inhibitors DMJ or KIF was added 8 h posttransfection to untreated or GPG-NH₂-treated cells. Treatment with CST increased the mass of gp160 due to the presence of additional glucoses on each glycan. CST also inhibited gp160 processing to gp41, but it did not prevent the action of GPG-NH₂ since faster-migrating gp160 products were still observed (Fig. 5C, lanes 1 to 4). Mannosidase inhibition had no influence on the effect of GPG-NH₂ (Fig. 5C, lanes 5 to 10). Taken together, these observations indicated that GPG-NH₂ affected gp160 within the ER, leading to a reduction in the number of N-linked glycans present on its polypeptide backbone.

Proteasome inhibition prevents GPG-NH₂-induced deglycosylation of gp160. Glycoproteins targeted for ERAD are deglycosylated in the cytoplasm by N-glycanase prior to proteasomal degradation. To determine whether the decrease in

gp160 glycan content and steady-state levels was a result of GPG-NH₂ targeting gp160 to the ERAD pathway, proteasomes were partially inhibited with LCT. LCT was added 10 h posttransfection, and the steady-state levels of gp160 were analyzed by immunoblotting. The partial proteasome inhibition by LCT, in the presence of GPG-NH₂, stabilized the completely glycosylated gp160 enabling its processing to gp41 and allowed the visualization of smaller gp160 degradation intermediates (Fig. 6A, top panel, compare lane 2 to lanes 4 and 6). Similarly, proteasome inhibition prevented the slight deglycosylation of LAMP-1 in GPG-NH₂-treated cells (Fig. 6A, bottom panel, compare lane 2 to lanes 4 and 6). Fully glycosylated gp160 could also be rescued by the proteasome inhibitor epoxomicin (Fig. 6B, compare lanes 2 to 4). The rescue of fully glycosylated gp160, by proteasome inhibition, showed that the GPG-NH₂-induced glycan deficiency was caused by glycan removal and not inefficient addition. Furthermore, proteasomal inhibition increased the steady-state levels of gp160 in the presence of GPG-NH₂. This shows that GPG-NH₂ targets gp160 toward ERAD, resulting in its proteasome-mediated retrotranslocation to the cytoplasm, where it is deglycosylated prior to degradation.

To examine whether the deglycosylated fractions of gp160 that accumulate in the presence of GPG-NH₂ are membrane bound or have been released into the cytosol upon retrotranslocation from the ER, membrane fractions were isolated after cell fractionation. Both gp160 and gp41 derived from cell homogenates of untreated and GPG-NH₂-treated cells were found entirely in the membrane fractions (Fig. 6C, lanes 3 to 6). Further alkaline extraction of the cellular membranes indicated that the gp160 remained an integral membrane protein after treatment with GPG-NH₂ (Fig. 6C, lanes 7 to 10). As a positive control for integral membrane proteins, gp41 and calnexin were monitored and found only in the membrane pellet after alkaline extraction. Therefore, the gp160 that accumulates after GPG-NH₂ treatment appears to remain associated with the membrane.

GPG-NH₂ requires the native gp160 signal sequence to facilitate its targeting to ERAD. In general, substrates targeted for ERAD are improperly folded. This raises the possibility that GPG-NH₂ acts adversely on a unique step in gp160 maturation. During maturation, gp160 undergoes a rare posttranslational cleavage of its signal sequence, which contributes to its prolonged presence within the ER. The delayed cleavage is partially due to several positively charged amino acids in the n-region of the signal sequence (24, 25). To investigate whether the positively charged n-region was important for the action of GPG-NH₂, a mutant version of gp160 (Δ nSS-gp160) was created lacking the entire n-region of its signal sequence (Fig. 7A). Upon cellular expression Δ nSS-gp160 had a molecular mass of 160 kDa and was processed into gp41. This indicated that the mutant was still targeted to the ER and transported to the Golgi (Fig. 7B, upper and lower panels, lanes 4 to 7). After a longer exposure, a fraction of Δ nSS-gp160 appeared to remain in the cytoplasm as a band corresponding to nonglycosylated gp160 (Fig. 7B, lower panel, lanes 4 to 7, ~90 kDa). Strikingly, the fully glycosylated ER-targeted Δ nSS-gp160 was completely unaffected by GPG-NH₂ treatment even at concentrations up to 500 μ M (Fig. 7B, upper and lower panels, compare lanes 1 to 3 to lanes 4 to 7). To ensure the

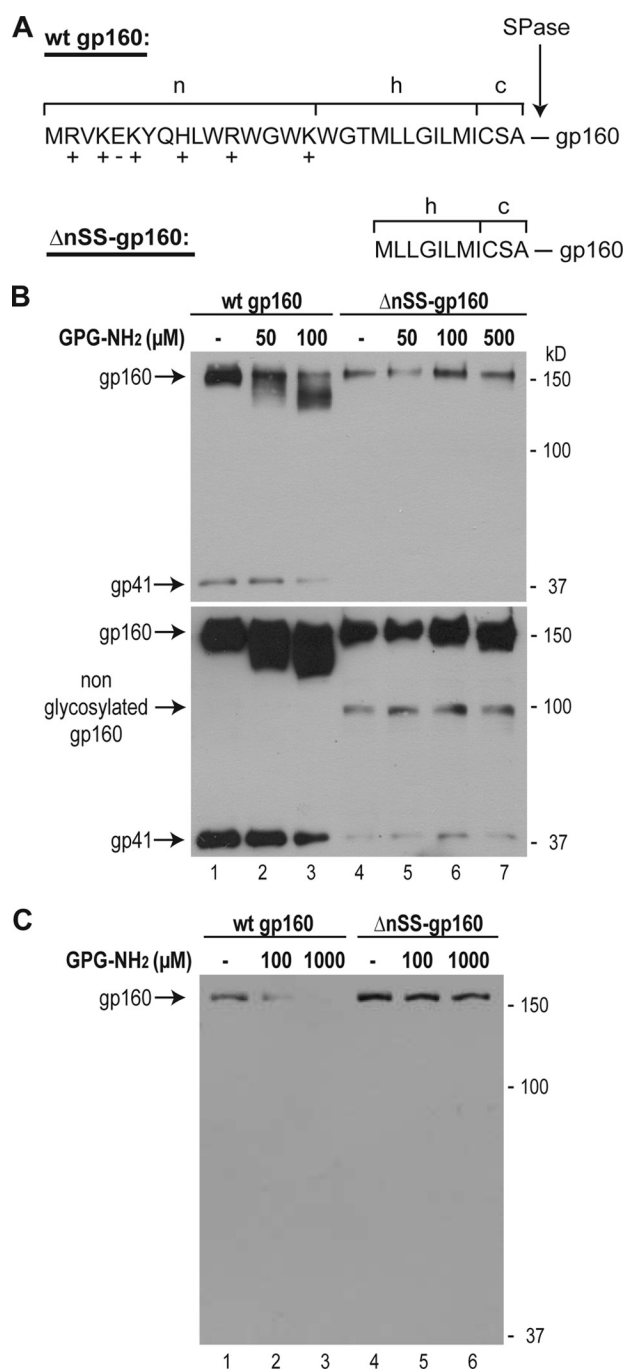


FIG. 7. GPG-NH₂ depends on the native gp160 signal sequence to target gp160 for ERAD. (A) The amino acid sequence corresponding to the signal sequence from the HIV-1 Env precursor protein gp160 containing its native signal sequence (wild-type gp160) and the truncated signal sequence (Δ nSS-gp160). The hydrophilic (n), hydrophobic (h), and C-terminal (c) regions, as well as the positively (+) and negatively (-) charged residues and the cleavage site for signal peptidase (SPase), are indicated. (B) Immunoblot of cell lysates from HeLa-tat III cells transfected with either wild-type gp160 or Δ nSS gp160, cultured in the indicated concentrations of GPG-NH₂, harvested at 20 h posttransfection, and probed with antibodies against gp41. Both a shorter exposure (upper panel) and a longer exposure (bottom panel) of the same immunoblot are shown. (C) Same as for panel B except that 0.3 μ g of vector expressing wild-type gp160 and 1 μ g of vector expressing Δ nSS-gp160 were used for transfection to reach similar expression levels of the respective proteins. wt, wild type.

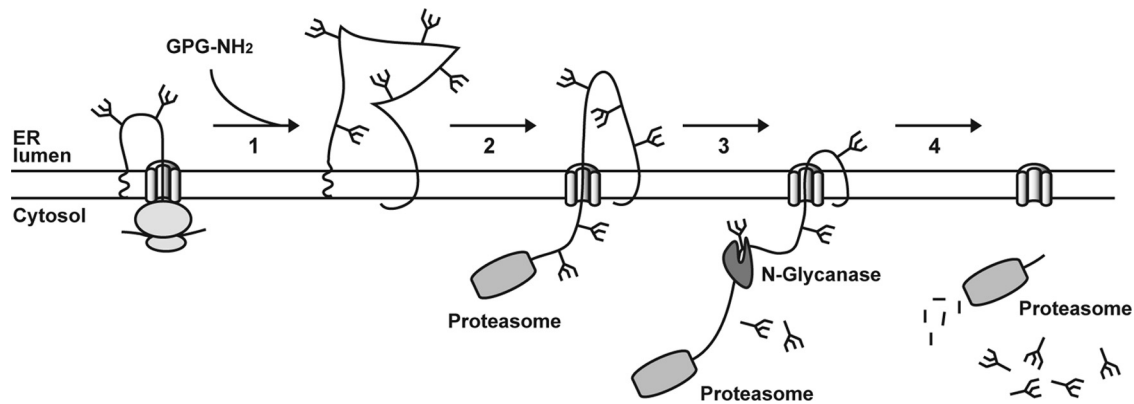


FIG. 8. Proposed model of how GPG-NH₂ targets gp160 to ERAD. Initially, gp160 is cotranslationally translocated into the ER. (Arrow 1) The presence of GPG-NH₂ or its metabolites prevents the proper folding of gp160, while its signal sequence remains attached. The improper folding of gp160 causes it to be targeted for ERAD. (Arrow 2) gp160 is then retrotranslocated to the cytoplasm in a proteasome-mediated fashion. The polypeptide remains integrated into the ER membrane, likely through its transmembrane region, while (arrow 3) it is deglycosylated by the cytosolic N-glycanase prior to (arrow 4) degradation by the proteasome.

lower expression level of Δ nSS-gp160 did not mask the effect of GPG-NH₂, the vector expressing wild-type gp160 was titrated during the transfection to reach the expression level of Δ nSS-gp160. It was found that that the wild-type gp160 was still affected while the Δ nSS-gp160 remained unaffected even up to 1,000 μ M GPG-NH₂ (Fig. 7C). These data further indicate that GPG-NH₂ targets gp160 for ERAD by altering a specific step in its maturation process that involves its native signal sequence.

DISCUSSION

HIV-1 readily escapes host immune responses and antiretroviral drugs due to its ability to mutate and adapt to the environment in which it replicates. To counteract this property, the available HIV-1 therapies utilize combinations of drugs targeting the viral RT, protease, and recently also the integrase and viral envelope fusion with the host cell plasma membrane (9, 19, 33). However, HIV-1 still poses a significant therapeutic problem as it continues to evolve multidrug resistance (20). Thus, development of new antiviral compounds with different modes of action from those currently available drugs is necessary to effectively combat HIV-1 infection.

In the present study, we uncovered a previously unexplored mechanism for suppressing HIV-1 propagation using the drug GPG-NH₂. The presence of GPG-NH₂ during HIV-1 replication drastically reduced HIV-1 particle infectivity by decreasing the viral incorporation of Env. Our findings are summarized into a model (Fig. 8) in which the viral Env incorporation was reduced due to the specific ability of GPG-NH₂ to direct maturing Env for degradation via the ERAD pathway. Consequently, gp160 is retrotranslocated from the ER lumen into the cytoplasm, where it is deglycosylated prior to its degradation. This correlates with the proteasomal requirement for the observed decrease in gp160 steady-state levels, processing, N-linked glycan status, and subsequently its molecular weight.

The feasibility of developing a drug capable of targeting a specific substrate to the ERAD pathway increases when the substrate has a prolonged ER residency and possesses

unique steps in its maturation process that can be disrupted. gp160 undergoes a rare posttranslational signal sequence cleavage in the ER that occurs after substantial maturation and disulfide bond formation (21). The abnormally late removal of the signal sequence is directed in part by several positively charged residues in its n-region that also contribute to the prolonged existence of gp160 within the ER (24, 25). Consequently, the native gp160 signal sequence could extend the time period for GPG-NH₂ to act on gp160, leading to its pronounced sensitivity to the drug. To examine the significance of the positively charged region within the signal sequence, for the effect of GPG-NH₂ on gp160, the entire n-region was deleted. The effects of GPG-NH₂ on this construct were entirely abolished, supporting the view that the prolonged ER residency of gp160 contributes to its enhanced GPG-NH₂ sensitivity. Alternatively, GPG-NH₂ may interact directly with the n-region of the signal sequence and adversely affect the maturation of gp160 by disrupting the signal sequence insertion into the ER membrane. However, the removal of the n-region is predicted in silico by SignalP 3.0 (7, 29, 30) to create a signal anchor sequence. This scenario rather indicates that GPG-NH₂ disrupts gp160 maturation by interacting with the mature n terminus of gp160 after signal sequence cleavage.

The effect of GPG-NH₂ has been shown to be restricted to glycoproteins, since gp160, LAMP-1, and an unspecified glycoprotein (~150 kDa) were affected, while the nonglycosylated ER resident protein calnexin and the viral cytosolic proteins p55Gag and p24 were not. However, a great diversity was observed in the glycoprotein susceptibility to GPG-NH₂ treatment, indicating a certain degree of specificity. The endogenous glycoprotein LAMP-1, as well as the concanavalin A-detected glycoproteins, exhibited a significantly lower sensitivity to GPG-NH₂ than gp160, with only slight effects being observed at 0.5 to 1 mM. These findings imply that GPG-NH₂ acts selectively among glycoproteins, where gp160 is more sensitive to the drug than endogenous proteins. In agreement with this is the finding that GPG-NH₂ treatment did not induce the UPR. Furthermore, the specificity of GPG-NH₂ was readily

apparent by its inability to target gp160 with an N-terminal truncated signal sequence to ERAD.

The use of peptides for therapy raises concerns regarding their short viability due to their high susceptibility to proteases. However, GPG-NH₂ has been found to gain its antiviral activity toward HIV-1 upon being metabolized to α -hydroxy glycineamide via the intermediate glycineamide (2, 5, 6; unpublished data). Furthermore, α -hydroxy glycineamide has been found to exhibit the same ability as GPG-NH₂ to reduce Env incorporation into HIV-1 particles, but at a higher efficiency (unpublished data).

We therefore believe this compound offers a potential lead for the development of a new type of drugs for use against HIV-1 and other pathogens. These drugs would be utilized to specifically target the removal of essential pathogenic substrates using the preexisting cellular degradation machinery. The therapeutic benefits of this approach are twofold. First, degradation of an essential pathogenic component would reduce the ability of the pathogen to propagate. Second, enhanced degradation of the foreign protein would lead to increased antigen production for major histocompatibility complex class I presentation, improving the chances of eliciting an immune response to infected cells (38).

Decreasing HIV-1 particle infectivity by targeting Env maturation, using general glucose trimming inhibitors such as CST or deoxynojirimycin, has been tried by others (14). These compounds do not target glycoproteins to the ERAD pathway, nor do they have specificity for viral glycoproteins. Although these inhibitors suppressed HIV-1 replication in vitro by preventing gp160 processing in the Golgi, they did not diminish Env incorporation or enhance its degradation (14). Ultimately, the lack of specificity for these glucosidase inhibitors has prevented their development for therapeutics. We demonstrate here that a drug can selectively induce the degradation of the HIV-1 envelope glycoprotein by targeting it for ERAD, thus limiting its incorporation into viral particles and thereby reducing their infectivity.

ACKNOWLEDGMENTS

We thank the original donors and the NIH AIDS Research and Reference Reagent Program, Division of AIDS, NIAID, for the cell lines HeLa-tat III from William Haseltine and Ernest Terwilliger, ACH-2 from Thomas Folks, SupT1 from James Hoxie, and TZM-bl from John C. Kabbes, Xiaoyun Wu, and Transzyme, Inc. We are grateful for the anti-gp41 antibody (Chessie 8) from George Lewis and the plasmid pNL4-3 from Malcolm Martin. We also thank Jorma Hinkula for kindly providing the anti-p24 (EF7) and anti-V3 (F58/H3) and (p4/D10) antibodies.

This study was supported by grants from the Swedish Medical Foundation (grant K2000-06X-09501-10B), the Swedish International Development Cooperation Agency, SIDA (grant HIV-2006-050), and by Tripep AB. A.V. is a founder of Tripep AB and a member of its board. D.N.H. is supported by a Public Health Service (grant CA79864).

REFERENCES

1. Abacioglu, Y. H., T. R. Fouts, J. D. Laman, E. Claassen, S. H. Pincus, J. P. Moore, C. A. Roby, R. Kamin-Lewis, and G. K. Lewis. 1994. Epitope mapping and topology of baculovirus-expressed HIV-1 gp160 determined with a panel of murine monoclonal antibodies. *AIDS Res. Hum. Retrovir.* **10**:371–381.
2. Abdurahman, S., A. Vegvari, M. Levi, S. Høglund, M. Hogberg, W. Tong, I. Romero, J. Balzarini, and A. Vahlne. 2009. Isolation and characterization of a small antiretroviral molecule affecting HIV-1 capsid morphology. *Retrovirology* **6**:34.
3. Adachi, A., H. E. Gendelman, S. Koenig, T. Folks, R. Willey, A. Rabson, and M. A. Martin. 1986. Production of acquired immunodeficiency syndrome-associated retrovirus in human and nonhuman cells transfected with an infectious molecular clone. *J. Virol.* **59**:284–291.
4. Ahner, A., and J. L. Brodsky. 2004. Checkpoints in ER-associated degradation: excuse me, which way to the proteasome? *Trends Cell Biol.* **14**:474–478.
5. Andersson, E., P. Horal, A. Jejcic, S. Høglund, J. Balzarini, A. Vahlne, and B. Svennerholm. 2005. Glycine-amide is an active metabolite of the antiretroviral tripeptide glycyL-prolyl-glycine-amide. *Antimicrob. Agents Chemother.* **49**:40–44.
6. Balzarini, J., E. Andersson, D. Schols, P. Proost, J. Van Damme, B. Svennerholm, P. Horal, and A. Vahlne. 2004. Obligatory involvement of CD26/dipeptidyl peptidase IV in the activation of the antiretroviral tripeptide glycyL-prolyl-glycineamide (GPG-NH₂). *Int. J. Biochem. Cell Biol.* **36**:1848–1859.
7. Bendtsen, J. D., H. Nielsen, G. von Heijne, and S. Brunak. 2004. Improved prediction of signal peptides: SignalP 3.0. *J. Mol. Biol.* **340**:783–795.
8. Broliden, P. A., K. Ljunggren, J. Hinkula, E. Norrby, L. Akerblom, and B. Wahren. 1990. A monoclonal antibody to human immunodeficiency virus type 1 which mediates cellular cytotoxicity and neutralization. *J. Virol.* **64**:936–940.
9. Carmona, R., L. Perez-Alvarez, M. Munoz, G. Casado, E. Delgado, M. Sierra, M. Thomson, Y. Vega, E. Vazquez de Parga, G. Contreras, L. Medrano, and R. Najera. 2005. Natural resistance-associated mutations to Enfuvirtide (T20) and polymorphisms in the gp41 region of different HIV-1 genetic forms from T20 naive patients. *J. Clin. Virol.* **32**:248–253.
10. Clouse, K. A., D. Powell, I. Washington, G. Poli, K. Strebel, W. Farrar, P. Barstad, J. Kovacs, A. S. Fauci, and T. M. Folks. 1989. Monokine regulation of human immunodeficiency virus-1 expression in a chronically infected human T cell clone. *J. Immunol.* **142**:431–438.
11. Daniels, R., S. Svedine, and D. N. Hebert. 2004. N-linked carbohydrates act as luminal maturation and quality control protein tags. *Cell Biochem. Biophys.* **41**:113–138.
12. Derdeyn, C. A., J. M. Decker, J. N. Sfakianos, X. Wu, W. A. O'Brien, L. Ratner, J. C. Kappes, G. M. Shaw, and E. Hunter. 2000. Sensitivity of human immunodeficiency virus type 1 to the fusion inhibitor T-20 is modulated by coreceptor specificity defined by the V3 loop of gp120. *J. Virol.* **74**:8358–8367.
13. Devito, C., M. Levi, K. Broliden, and J. Hinkula. 2000. Mapping of B-cell epitopes in rabbits immunised with various gag antigens for the production of HIV-1 gag capture ELISA reagents. *J. Immunol. Methods* **238**:69–80.
14. Dwek, R. A., T. D. Butters, F. M. Platt, and N. Zitzmann. 2002. Targeting glycosylation as a therapeutic approach. *Nat. Rev. Drug Discov.* **1**:65–75.
15. Earl, P. L., B. Moss, and R. W. Doms. 1991. Folding, interaction with GRP78-BiP, assembly, and transport of the human immunodeficiency virus type 1 envelope protein. *J. Virol.* **65**:2047–2055.
16. Ellgaard, L., and A. Helenius. 2003. Quality control in the endoplasmic reticulum. *Nat. Rev. Mol. Cell. Biol.* **4**:181–191.
17. Gomez, C., and T. J. Hope. 2005. The ins and outs of HIV replication. *Cell Microbiol.* **7**:621–626.
18. Horal, P., W. W. Hall, B. Svennerholm, J. Lycke, S. Jeansson, L. Rymo, M. H. Kaplan, and A. Vahlne. 1991. Identification of type-specific linear epitopes in the glycoproteins gp46 and gp21 of human T-cell leukemia viruses type I and type II using synthetic peptides. *Proc. Natl. Acad. Sci. USA* **88**:5754–5758.
19. Kalkut, G. 2005. Antiretroviral therapy: an update for the non-AIDS specialist. *Curr. Opin. Oncol.* **17**:479–484.
20. Kuritzkes, D. R. 2004. Preventing and managing antiretroviral drug resistance. *AIDS Patient Care STDS* **18**:259–273.
21. Land, A., D. Zonneveld, and I. Braakman. 2003. Folding of HIV-1 envelope glycoprotein involves extensive isomerization of disulfide bonds and conformation-dependent leader peptide cleavage. *FASEB J.* **17**:1058–1067.
22. Lee, K., W. Tirasophon, X. Shen, M. Michalak, R. Prywes, T. Okada, H. Yoshida, K. Mori, and R. J. Kaufman. 2002. IRE1-mediated unconventional mRNA splicing and S2P-mediated ATF6 cleavage merge to regulate XBP1 in signaling the unfolded protein response. *Genes Dev.* **16**:452–466.
23. Lee, R. J., C. W. Liu, C. Harty, A. A. McCracken, M. Latterich, K. Romisch, G. N. DeMartino, P. J. Thomas, and J. L. Brodsky. 2004. Uncoupling retrotranslocation and degradation in the ER-associated degradation of a soluble protein. *EMBO J.* **23**:2206–2215.
24. Li, Y., L. Luo, D. Y. Thomas, and C. Y. Kang. 1994. Control of expression, glycosylation, and secretion of HIV-1 gp120 by homologous and heterologous signal sequences. *Virology* **204**:266–278.
25. Li, Y., L. Luo, D. Y. Thomas, and C. Y. Kang. 2000. The HIV-1 Env protein signal sequence retards its cleavage and downregulates the glycoprotein folding. *Virology* **272**:417–428.
26. Lu, M., S. C. Blacklow, and P. S. Kim. 1995. A trimeric structural domain of the HIV-1 transmembrane glycoprotein. *Nat. Struct. Biol.* **2**:1075–1082.
27. McCune, J. M., L. B. Rabin, M. B. Feinberg, M. Lieberman, J. C. Kosek, G. R. Reyes, and I. L. Weissman. 1988. Endoproteolytic cleavage of gp160 is required for the activation of human immunodeficiency virus. *Cell* **53**:55–67.
28. Meusser, B., C. Hirsch, E. Jarosch, and T. Sommer. 2005. ERAD: the long road to destruction. *Nat. Cell Biol.* **7**:766–772.

29. **Nielsen, H., J. Engelbrecht, S. Brunak, and G. von Heijne.** 1997. Identification of prokaryotic and eukaryotic signal peptides and prediction of their cleavage sites. *Protein Eng.* **10**:1–6.
30. **Nielsen, H., and A. Krogh.** 1998. Prediction of signal peptides and signal anchors by a hidden Markov model. *Proc. Int. Conf. Intell. Syst. Mol. Biol.* **6**:122–130.
31. **Otteken, A., and B. Moss.** 1996. Calreticulin interacts with newly synthesized human immunodeficiency virus type 1 envelope glycoprotein, suggesting a chaperone function similar to that of calnexin. *J. Biol. Chem.* **271**:97–103.
32. **Schwartz, S., B. K. Felber, E. M. Fenyo, and G. N. Pavlakis.** 1990. Env and Vpu proteins of human immunodeficiency virus type 1 are produced from multiple bicistronic mRNAs. *J. Virol.* **64**:5448–5456.
33. **Semenova, E. A., C. Marchand, and Y. Pommier.** 2008. HIV-1 integrase inhibitors: update and perspectives. *Adv. Pharmacol.* **56**:199–228.
34. **Smith, S. D., M. Shatsky, P. S. Cohen, R. Warnke, M. P. Link, and B. E. Glader.** 1984. Monoclonal antibody and enzymatic profiles of human malignant T-lymphoid cells and derived cell lines. *Cancer Res.* **44**:5657–5660.
35. **Su, J., E. Andersson, P. Horal, M. H. Naghavi, A. Palm, Y. P. Wu, K. Eriksson, M. Jansson, H. Wigzell, B. Svennerholm, and A. Vahlne.** 2001. The nontoxic tripeptide glycyl-prolyl-glycine amide inhibits the replication of human immunodeficiency virus type 1. *J. Hum. Virol.* **4**:1–7.
36. **Su, J., M. H. Naghavi, A. Jejcic, P. Horal, Y. Furuta, Y. P. Wu, S. L. Li, W. W. Hall, L. Goobar-Larsson, B. Svennerholm, and A. Vahlne.** 2001. The tripeptide glycyl-prolyl-glycine amide does not affect the early steps of the human immunodeficiency virus type 1 replication. *J. Hum. Virol.* **4**:8–15.
37. **Terwilliger, E., J. Proulx, J. Sodroski, and W. A. Haseltine.** 1988. Cell lines that express stably env gene products from three strains of HIV-1. *J. Acquir. Immune Defic. Syndr.* **1**:317–323.
38. **Wu, Y., and T. J. Kipps.** 1997. Deoxyribonucleic acid vaccines encoding antigens with rapid proteasome-dependent degradation are highly efficient inducers of cytolytic T lymphocytes. *J. Immunol.* **159**:6037–6043.
39. **Ye, Y., H. H. Meyer, and T. A. Rapoport.** 2001. The AAA ATPase Cdc48/p97 and its partners transport proteins from the ER into the cytosol. *Nature* **414**:652–656.